SCIENTIFIC REPORTS
nature research

OPEN

Competing effects of soil fertility and toxicity on tropical greening

Joshua B. Fisher[1*], Naga V. Perakalapudi[2], Benjamin L. Turner[3], David S. Schimel[1] & Daniela F. Cusack[3,4]

Tropical forests are expected to green up with increasing atmospheric CO_2 concentrations, but primary productivity may be limited by soil nutrient availability. However, rarely have canopy-scale measurements been assessed against soil measurements in the tropics. Here, we sought to assess remotely sensed canopy greenness against steep soil nutrient gradients across 50 1-ha mature forest plots in Panama. Contrary to expectations, increases in *in situ* extractable soil phosphorus (P) and base cations (K, Mg) corresponded to declines in remotely sensed mean annual canopy greenness ($r^2 = 0.77–0.85$; $p < 0.1$), controlling for precipitation. The reason for this inverse relationship appears to be that litterfall also increased with increasing soil P and cation availability ($r^2 = 0.88–0.98$; $p < 0.1$), resulting in a decline in greenness with increasing annual litterfall ($r^2 = 0.94$; $p < 0.1$). As such, greater soil nutrient availability corresponded to greater leaf turnover, resulting in decreased greenness. However, these decreases in greenness with increasing soil P and cations were countered by increases in greenness with increasing soil nitrogen (N) ($r^2 = 0.14$; $p < 0.1$), which had no significant relationship with litterfall, likely reflecting a direct effect of soil N on leaf chlorophyll content, but not on litterfall rates. In addition, greenness increased with extractable soil aluminum (Al) ($r^2 = 0.97$; $p < 0.1$), but Al had no significant relationship with litterfall, suggesting a physiological adaptation of plants to high levels of toxic metals. Thus, spatial gradients in canopy greenness are not necessarily positive indicators of soil nutrient scarcity. Using a novel remote sensing index of canopy greenness limitation, we assessed how observed greenness compares with potential greenness. We found a strong relationship with soil N only ($r^2 = 0.65$; $p < 0.1$), suggesting that tropical canopy greenness in Panama is predominantly limited by soil N, even if plant productivity (e.g., litterfall) responds to rock-derived nutrients. Moreover, greenness limitation was also significantly correlated with fine root biomass and soil carbon stocks ($r^2 = 0.62–0.71$; $p < 0.1$), suggesting a feedback from soil N to canopy greenness to soil carbon storage. Overall, these data point to the potential utility of a remote sensing product for assessing belowground properties in tropical ecosystems.

Tropical forests are the 'lungs' of our planet, absorbing and storing the largest carbon stocks of all terrestrial ecosystems[1–4]. They are also the source of among the largest uncertainties to projections of Earth's climate, due to their poorly understood responses to changes in CO_2, climate, land use, and nutrient cycling[5–9]. Numerous modeling studies have suggested that tropical forest productivity is increasing[5,6], and present day observational indicators from space suggest that the tropics are greening likely due to CO_2 fertilization, in the face of increasing pressure from droughts and disturbance[10–16].

Despite the apparent greening of the tropics, it is well-known that there is widespread nutrient limitation to net primary productivity[17–23]. The extent, nature, and impacts of soil nutrient availability are debated, however. Some studies show strong tropical forest responses to phosphorus (P)[24–30], others to nitrogen (N)[31–33], some indicate strong influence of multiple macro-nutrients on tropical forest processes[17,22,34–36], and others suggest that micronutrients and/or base cations drive key ecosystem carbon processes[37–43]. These studies have also linked soil nutrients to a wide range of different tropical forest carbon cycle responses, including litterfall rates, basal growth, root production, and soil decomposition, for example, with responses varying by tree age and size[20,24,30,37,44,45].

[1]Jet Propulsion Laboratory, California Institute of Technology, 4800 Oak Grove Drive, Pasadena, CA, 91109, USA. [2]Department of Astronautical Engineering, University of Southern California, 854 Downey Way, Los Angeles, CA, 90089, USA. [3]Smithsonian Tropical Research Institute, Apartado 0843-03092, Balboa, Ancon, Panama. [4]Department of Ecosystem Science and Sustainability, Colorado State University, Campus Delivery 1476, Fort Collins, CO, 80523, USA. *email: jbfisher@jpl.nasa.gov

The reason for such different results is that tropical ecosystems are both extremely diverse and challenging to work in, such that ground data at specific points cannot adequately capture the dynamics of variation across the biome as a whole[1,21,30,46]. Remote sensing data, on the other hand, have the potential to scale across landscapes, but lack insight from ground-scale controls over canopy properties[1,9]. Moreover, studies of remote sensing observations and those of *in situ* soil measurements have been done largely in isolation of one another. As such, there exists a critical gap in our understanding of how soil properties manifest in canopy-scale properties across tropical landscapes.

We are currently in a golden age of satellite remote sensing of terrestrial vegetation. Decades of work with Landsat, AVHRR, and MODIS have yielded a wealth of data and insights across multiple properties from albedo and surface temperature to greenness, as well as a host of higher-order datasets for productivity, evapotranspiration, nutrient limitation, and mycorrhizal association, for example[19,47–51]. Although the potential is large for ecosystem assessment of soil nutrient linkages to canopy properties with these data, these remote sensing data products have not been partnered with a similarly large-scale soils database from the tropics.

One of the most comprehensive tropical soils datasets to date has been collected over a decade by the Smithsonian Tropical Research Institute (STRI) across 50 1-ha plots in lowland tropical forest sites across the Isthmus of Panama, covering a wide range in geology, climate, and biodiversity[43,52–54]. The strong diversity of environmental conditions across the study area makes observed trends broadly applicable to much larger geographical ranges, and the relatively large-scale of the plots makes this dataset compatible with remote sensing attributes. Particularly characteristic to these sites is that, although they fall along a distinct precipitation gradient, the diverse geology drives variability in soil nutrients such that they are only weakly or not at all correlated with precipitation, making this dataset uniquely suited for disentangling effects of precipitation from soil properties. The STRI dataset is an ideal source with which to combine terrestrial vegetation remote sensing products to assess below- and above-ground coupling, and soil nutrient controls on canopy-scale properties.

The objective of this study was to assess remotely sensed canopy properties, particularly gradients of greenness and derived products, across a large-scale tropical gradient in soil nutrient availability and other chemical properties. We tested predictions that soil nutrients and soil carbon stocks would be positively related to canopy properties related to productivity, such as greenness. Such relationships would reflect the control of soil nutrients over plant productivity, and subsequent control of plants over carbon inputs to ecosystems. The overall approach was to enable identification of potential couplings between belowground and aboveground measurements, disentangling effects of precipitation from soil properties.

Methods

Field measurements. All plots were in lowland tropical forests (elevation 10–410 m above sea level) and included old growth primary and mature secondary forests across a precipitation gradient in Panama[55]. The climate is tropical monsoon, with a mean annual temperature of 26 °C and mean monthly temperature variation of <1 °C during the year[52,55,56]. The wetter Caribbean coast receives 4000 mm y^{-1} MAP and has a shorter dry season (~115 days) compared with the drier Pacific coast, which receives 1750 mm y^{-1} MAP and has a longer dry season (~150 days). Meteorological data were measured at each site. Radiation is inversely proportional to precipitation;[57–59] and, given low temperature variability, we assessed each site for precipitation normalization.

Soils were collected during the 8-month wet season as described in Turner, *et al.*[60]. Soil properties, litterfall, and aboveground biomass were measured using standard protocols, as previously reported[30,43,52–55]. In brief, total soil C, N, P, resin-extractable P, extractable base cations, pH, soil texture, root biomass, and bulk density were measured to 1 m depth in 1-ha plots at each site (Supplementary Fig. 1) sampling both across the spatial variation within plots, and in soil pits (1.8 m deep) outside the edge of each plot.

The soils developed on a range of geological substrates[54,55,61,62], including volcanic (basalt, andesite, agglomerate, rhyolitic tuff) and marine sedimentary (limestone, calcareous sandstone, siltstone, mudstone) lithologies. As a result, soils have marked variation in fertility[53,54] and soil order, including Inceptisols, Mollisols, Alfisols, Ultisols, and Oxisols. Soil nutrients such as P spanned high and low fertility across multiple soil types. Statistics are shown here by soil order across plots except for N, P, Ca, and Zn.

Aboveground dry biomass (AGB) for all trees >10 cm in diameter at breast height (DBH) was estimated in each of the plots using allometric equations. Methodological details and examination of errors have been published[63], with the most recent DBH decadal census used for this paper[30]. Litterfall biomass was collected at a subset of 8 sites biweekly for one year as described in Cusack, *et al.*[43]. All soils, AGB, and litterfall data are published as an online supplementary file in Cusack, *et al.*[43]. There were no significant differences among plots for aboveground biomass, canopy cover, species composition, and successional stage (all mature trees).

Remote sensing. We processed and analyzed data from 10 instruments on 8 different satellites, yielding a total of >70 different data products (Supplementary Fig. 1). The instruments and satellites included: Enhanced Thematic Mapper Plus (ETM+), Operational Land Imager (OLI), and Thermal Infrared Sensor (TIRS) on Landsat 7 and 8; MODerate resolution Imaging Spectroradiometer (MODIS) on Terra and Aqua; radar and radiometer on Soil Moisture Active Passive (SMAP); three high-resolution spectrometers on the Orbiting Carbon Observatory 2 (OCO-2); Geoscience Laser Altimeter System (GLAS) on Ice, Cloud, and land Elevation Satellite (ICESat); and, Hyperion on Earth Observing-1 (EO-1). Data were processed for an annual summary statistic for the most recent year (2016), except where otherwise available (e.g., ICESat, 2005).

Landsat 7 and 8: ETM+, OLI, TIRS. ETM+, OLI, and TIRS on Landsat 7 and 8 recorded measurements in 11 spectral bands (0.43–12.51 μm). We processed and analyzed data products for Normalized Difference Vegetation Index (NDVI), Enhanced Vegetation Index (EVI), Albedo, and Land Surface Temperature (LST)[64]. We acquired the data from the United States Geological Survey (USGS) Earth Resources Observation and Science (EROS)

Science Processing Architecture (ESPA) for both Landsat 7 (LE07, L1TP) and Landsat 8 (LE08, L1TP). Data were screened and masked for clouds based on the provided metadata and quality flags. Albedo for Landsat 7 was calculated through Top of Atmosphere (ToA) from bands 1, 3, 4, 5, and 7; and, for Landsat 8 from bands 2, 4, 5, 6, and 7 following Liang[65]. LST for Landsat 7 was calculated through surface reflectance from band 6; and, for Landsat 8 from band 10. Surface reflectance was converted to LST following: $L_\lambda = M_L Q_{cal} + A_L$, where L_λ is ToA spectral radiance (W m^{-2} $srad^{-1}$ μm^{-1}), M_L is a band-specific multiplicative rescaling factor from the metadata, A_L is a band-specific additive rescaling factor from the metadata, and Q_{cal} is quantized and calibrated standard product pixel value[66]. ToA brightness temperature (T, K) is: $T = \frac{K_2}{\log\left(\frac{K_1}{L_\lambda}+1\right)}$, where K_1 and K_2 are band-specific thermal conversion constants from the metadata. All Landsat products were available at 16-day time steps and 30 m spatial resolution.

Terra and Aqua: MODIS. MODIS on Terra and Aqua recorded measurements in 36 spectral bands (620 nm–965 nm and 3.66 μm–14.385 μm). We processed and analyzed data products for NDVI and EVI (MOD13Q1 V005, MYD13Q1 V005), gross primary productivity (GPP) (MOD17A2 V005, MOD17A3 V055, MYD17A2 V005), net primary productivity (NPP) (MOD17A3 V055, MYD17A3H V006), evapotranspiration (ET) (MOD16A2 V006), Leaf Area Index (LAI) and Fraction of Absorbed Photosynthetically Active Radiation (FAPAR) (MCD15AC3H V006), LST Day and Night (MOD11A1 V006, MYD11A1 V006), and Albedo Bands 1–10 Day and Night (MCD43A3 V005)[67]. Three ground sites were excluded from analyses of evapotranspiration due to pixel contamination from adjacency to open water (Plot 1: ocean; Plots 25 & 26: canal). We acquired the data from the USGS EROS Earth Observing System Data and Information System (EOSDIS) Land Processes DAAC for tiles h09v08 and h10v08. Data were screened and masked for clouds based on the provided metadata and quality flags. MODIS NDVI and EVI were available from daily measurements at 16 day temporal composites and 250 m spatial resolution; LAI, FAPAR, and Albedo at 4 day composites (LAI, FAPAR) or 16 day composites (Albedo) at 500 m; and, GPP, NPP, ET, and LST at 8 day composites (GPP, NPP, ET) or daily composites (LST) at 1 km. MODIS NPP and ET products were combined to produce the Canopy Greenness Limitation product described in Fisher, *et al.*[19]. Canopy greenness limitation (N.L.) is calculated from the ratio of NDVI to evapotranspiration (AET) normalized to a percentage, increasing further from the upper bound in the global scatterplot of average maximum paired AET and NDVI:

$$N.\,L. = \frac{paired_{max}\left(\frac{NDVI_x}{AET_x}\right) - paired_{max}\left(\frac{NDVI_{min}}{AET_{min}}\right)}{paired_{max}\left(\frac{NDVI_{max}}{AET_{max}}\right) - paired_{max}\left(\frac{NDVI_{min}}{AET_{min}}\right)}$$

where the $paired_{max}$ is for the quotient; the x subscript is for the given pixel; and the min and max are for across the entire data set to apply consistent global normalization.

SMAP: radar and radiometer. The SMAP radiometer recorded measurements at 1.41 Hz, and the radar at 1.26 Hz. We processed and analyzed data products for Soil Moisture (SM) and Albedo (SP3SMP V004, SPL3SMP E V001); Surface Soil Moisture (SSM), Root Zone Soil Moisture (RZSM), and LAI (SPL4SMGP V002); and, Net Ecosystem Exchange (NEE), Heterotrophic Respiration (Rh), Soil Organic Carbon (SOC), and GPP (SPL4CMDL V002)[68]. We acquired the data from the NASA Distributed Active Archive Center (DAAC) at the National Snow and Ice Data Center (NSIDC). SMAP data bins were extracted based on latitude and longitude from the EASE Grid projection and processed to WGS84 projection. Recommended retrieval quality flags were applied. Radar data were available only for 2015Q1-2. All SMAP products were available at daily time steps with SSM, RZSM, and LAI at 3 hourly time steps and 9 km spatial resolution; SM and Albedo were additionally available at 36 km (radiometer).

OCO-2: High-Resolution Spectrometers. The high-resolution spectrometers on OCO-2 recorded measurements at 0.76, 1.61 and 2.06 μm. We processed and analyzed data products for SIF generated from the Iterative Maximum a Posteriori Differential Optical Absorption Spectroscopy (IMAP-DOAS) preprocessor (L2IDP)[69]. We acquired the data from https://oco2.gesdisc.eosdis.nasa.gov/data/. OCO-2 data bins were extracted based on latitude and longitude from the EASE Grid projection and processed to WGS84 projection. Data were aggregated to monthly means for data/bands SIF757 and SIF771 following Sun, *et al.*[70]. OCO-2 SIF data were available at 16-day time steps and 36 km spatial resolution.

ICESat: GLAS. GLAS on ICESat recorded measurements from a full waveform LiDAR at 1.064 μm and 40 Hz. We processed and analyzed the vegetation canopy height product developed by Simard, *et al.*[71], which fused GLAS with MODIS and climate data to produce the product. We acquired the data using the Spatial Data Access Tool (SDAT) from the Oak Ridge National Laboratory (ORNL) DAAC. Data were provided in GeoTIFF format, pre-screened and quality controlled. ICESat canopy height data were available as a static map from 2005 at 1 km spatial resolution.

EO-1: Hyperion. Hyperion on EO-1 recorded measurements in 220 spectral bands ranging between 0.4–2.5 μm (SWIR and VNIR)[72]. We acquired the L1T data (systematically terrain-corrected) from Earth Explorer. Data were provided in GeoTIFF format. Forty-three bands were removed from the Hyperion cube as uncalibrated. Cloud screening was performed with bands 31, 51, and 133 using information on Julian day, sun elevation angle ($\cos\theta_s$), scaling factor, irradiance value ($ESUN_\lambda$), and Earth-Sun distance (d) from the metadata. Cloud-corrected

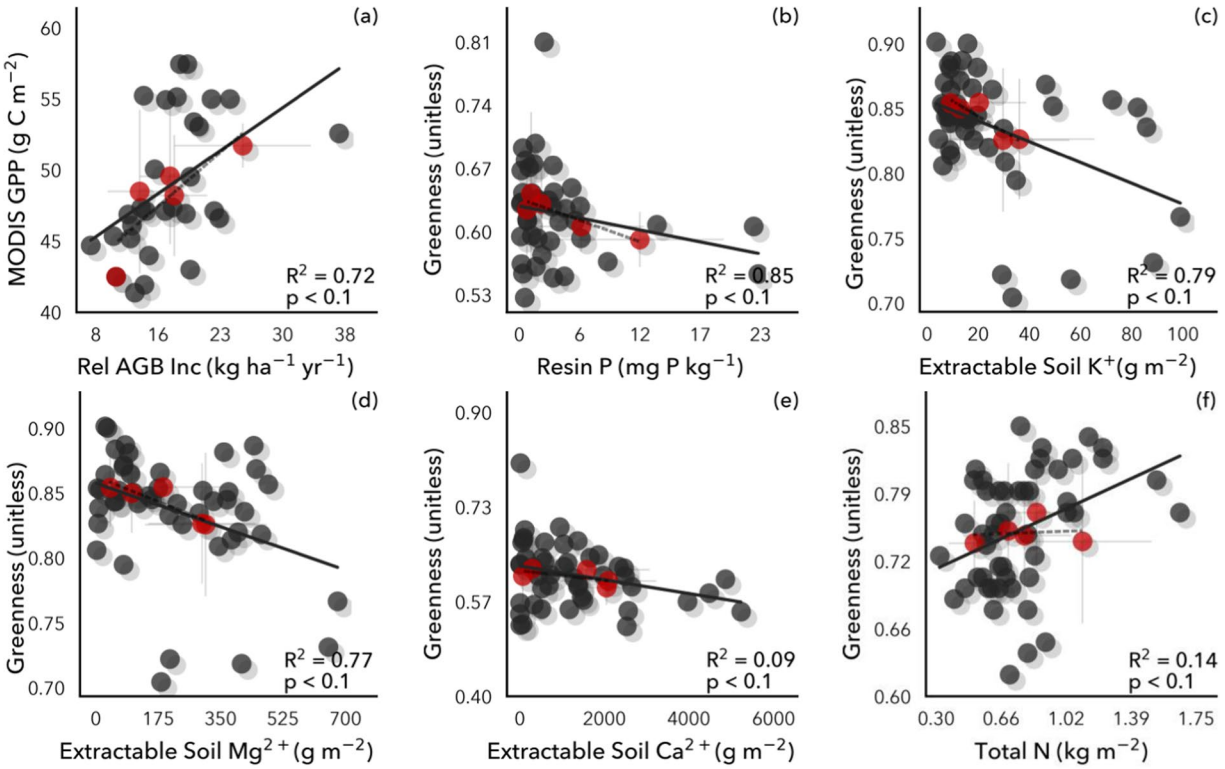

Figure 1. Remotely sensed canopy greenness was negatively correlated with *in situ* soil phosphorus (P) and cations (K, Mg, Ca), but positively correlated with *in situ* soil nitrogen (N) and aboveground biomass (AGB) increase. Individual plots (gray points, solid line) are aggregated by soil order (red points, dashed line; statistics shown).

radiance was converted to reflectance (ρ_p) using $\rho_p = \frac{\pi L_\lambda d^2}{ESUN_\lambda \cos\theta_s}$, where L_λ is spectral radiance at the sensor's aperture. Hyperion data were processed from images collected over 2002–2012 at 30 m spatial resolution.

Results and Discussion

We evaluated spatial gradients of *in situ* soil nutrients and chemical properties against remotely sensed canopy properties. Remotely sensed greenness and derived products such as GPP were correlated with *in situ* measurements of relative aboveground biomass increase ($r^2 = 0.72$; $p < 0.1$) (Fig. 1a). Contrary to expectations, as *in situ* extractable soil phosphorus (P) and base cations (calcium, Ca; potassium, K; magnesium, Mg) increased in availability across sites, remotely sensed mean annual canopy greenness decreased ($r^2 = 0.09$–0.79; $p < 0.1$) (Fig. 1b–e), controlling for climatic differences such as precipitation (Supplementary Fig. 2). Base cations (K and Mg) were strongly negatively correlated with NDVI (Landsat 8) ($r^2 = 0.79$ and 0.77), while Ca was weakly negatively correlated ($r^2 = 0.09$). We use the term "Greenness" instead of NDVI in the figures to facilitate translation to science communities unfamiliar with the remote sensing terminology. All statistics for Figs.1–4 can be found in Supplementary Table 1. Assessing only the wet season, the negative relationship between canopy greenness and Ca increased in strength ($r^2 = 0.91$), and remained similar for P, K, and Mg (Supplementary Fig. 2). It may be that these results could be even stronger than shown due to greenness saturation causing large point spreads at high values[73,74].

The inverse relationship between soil P and cations with canopy greenness likely results from a strong positive relationship between annual litterfall and soil P and cations ($r^2 = 0.88$–0.98; $p < 0.1$), indicating greater leaf turnover, and potentially shorter leaf lifespan, where soil nutrients are plentiful (Fig. 2b–f). Strong links between litterfall rates and soil fertility have been shown throughout the tropics, including Panama[20,37,75–77]. Accordingly, increasing litterfall was related to a strong decline in greenness ($r^2 = 0.94$; $p < 0.1$) (Fig. 2a). That is, litterfall increased with soil P and cation availability across the subset of sites with litterfall measurements, helping explain the broader negative relationship between canopy greenness and soil P and cations across all sites, as an increase in litterfall can lead to a brighter surface due to fewer canopy leaves[78,79]. At the same time, these decreases in greenness with increasing soil P and cations were countered by increases in greenness with increasing soil nitrogen (N) ($r^2 = 0.14$; $p < 0.1$) (Fig. 1f), with soil N not significantly correlated with litterfall (Fig. 2f), nor with soil P or cations.

Notably, we also found that canopy greenness was strongly positively correlated with extractable soil aluminum (Al) across soil orders ($r^2 = 0.97$; $p < 0.1$) (Fig. 3), which initially appears paradoxical as Al is toxic to plants[80–85]. Al was not significantly correlated with soil base cations nor with litterfall. In acidic soils, Al is solubized and can be a major factor limiting plant production[86], with increased Al concentrations in leaves associated with decreased photosynthetic rates and decreased foliar N, P, and other nutrients[87]. Extractable soil Al and manganese (Mn) were recently identified as the strongest constraints on canopy tree diameter growth for one of our Panama sites at mid-precipitation[88]. Aluminum toxicity can elicit plant responses in cell walls, plasma

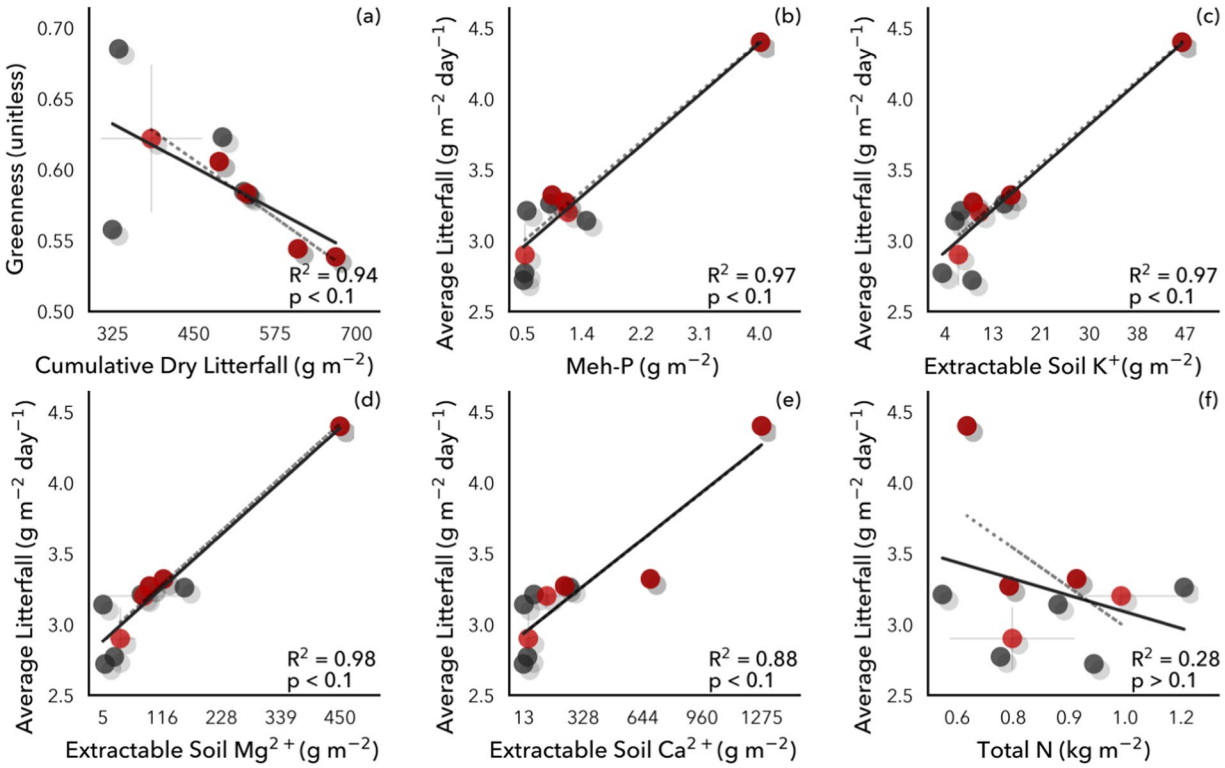

Figure 2. Litterfall was negatively correlated with remotely sensed canopy greenness, positively correlated with soil phosphorus (P) and cations (K, Mg, Ca), and had no relationship with soil nitrogen (N).

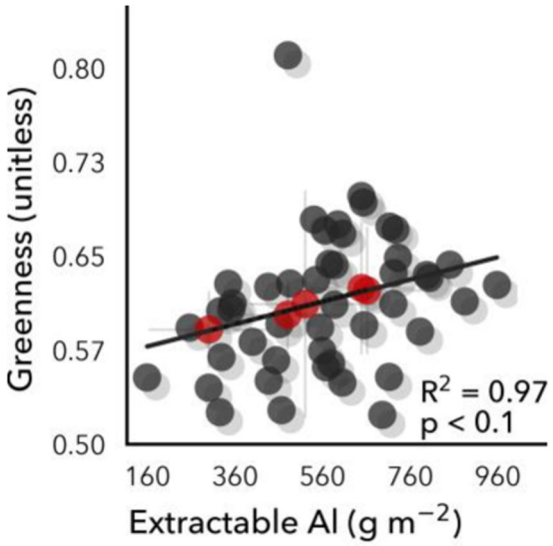

Figure 3. Remotely sensed canopy greenness was positively correlated with *in situ* extractable soil aluminum (Al), paradoxically given that Al is toxic to plants. It may be that tropical plants that have adapted to excess Al soils are relatively more productive than plants on less toxic soils because a significant amount of photosynthate is required to filter out the Al.

membranes, and symplasm[89], and metabolic changes like autophagy as defense responses[90], which can help repair plant tissue damages from Al toxicity. Thus, under elevated Al toxicity, plants may invest substantially in leaf repair, which could be related to longer leaf lifespans, changes in pigmentation, and/or leaf structural changes that could affect canopy reflectance properties. Thus, canopy greenness relationships with soil Al may result from change in leaf greenness not related to increased photosynthesis and growth, which canopy greenness is usually taken to indicate.

Spatial gradients in nutrients and greenness are not necessarily indicative of nutrient limitation[91]. Using a novel remote sensing index of canopy greenness limitation, we assessed how observed greenness compares with

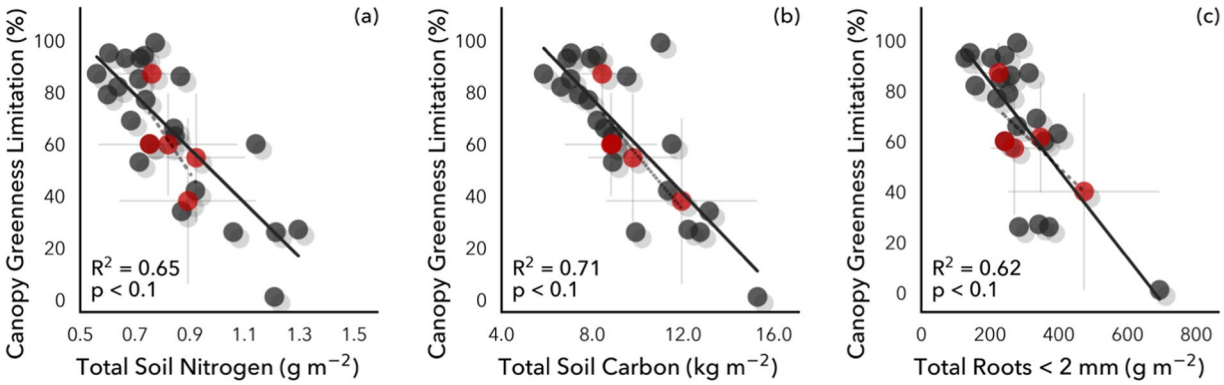

Figure 4. Remotely sensed canopy greenness limitation was strongly correlated with *in situ* (**a**) soil nitrogen, (**b**) soil carbon, and (**c**) total roots.

potential greenness based on energy and water availability at a broad scale[19]. We found a strong relationship with soil N only ($r^2 = 0.65$; $p < 0.1$) (Fig. 4a), suggesting that canopy greenness in tropical forests in Panama is predominantly driven by soil N, but not by other nutrients[23,76]. This could reflect the strong association between foliar N and chlorophyll content, with plants taking up additional N even in N-rich soils ("luxury consumption"). Also, total soil C ($r^2 = 0.71$; $p < 0.1$) and root biomass ($r^2 = 0.62$; $p < 0.1$) were strongly correlated with the remotely sensed canopy greenness limitation product (Fig. 4b,c), such that as the canopy approached maximum theoretical greenness, soil C and root biomass also increased. This relationship with soil C stocks could reflect greater root biomass and greater plant photosynthetic activity at higher soil N, both of which could contribute to soil C stocks[92–94]. This result contrasts with a fertilization experiment at one Panama site where added N alone had no effect on litterfall or stem growth rates, although N and P added together did appear to elevate productivity[77]. The links among soil N, canopy greenness, roots, and soil C may suggest a previously unmeasured input of C to soil via root exudates, which can be a significant sink of annual photosynthate, but are challenging to measure *in situ*[95]. The strong coupling between canopy and soil properties underscores the potential utility of remote sensing for assessing belowground properties in tropical ecosystems.

Our analysis thus far has aimed at exploring first-order relationships between soil properties and canopy greenness. Although this is just a first step, one may wish to see how these results can be integrated into mechanistic, process-based modeling systems, such as terrestrial biosphere models (TBMs) or Earth system models (ESMs)[96]. The need for nutrient processes, especially in the tropics, is well-stated[27,96–99]. Certainly, building these relationships into these types of models is beyond the scope of this paper. Still, our results provide comparative behaviors for the results of future model developments[100,101]. Numerous multi-variate statistical approaches can also assign weighting to the different controls on canopy greenness responses. These approaches include, for example, multi-variate regression, artificial neural networks, random forest, principal components analysis, and structural equation modeling. We have used these approaches extensively in previous analyses[102–104]. In this analysis, however, the data distribution statistical requirements for these approaches were not always satisfied, and, while the results largely reinforced what we already found, they often minimized interesting relationships with the micronutrients. Moreover, some approaches, such as structural equation modeling, require certain assumptions about fixed pathways, or known relationships, that must be defined. Yet, our results showed unexpected responses, such as decreasing greenness with increasing P and base cations. Ultimately, soil N was the only nutrient-based significant predictor of canopy greenness limitation.

Although it had already been established that the sites were situated such that soil properties were only weakly or not at all correlated with precipitation[43,52–54], we took additional measures to separate the influence of precipitation from soil properties on canopy characteristics[105–107]. First, we evaluated all data normalized by mean annual precipitation (Supplementary Fig. 2). Second, we assessed only wet season canopy properties from the remote sensing data (and *in situ* data, where appropriate; i.e., litterfall), though there were fewer cloud-free remote sensing data in the wet season-only analysis (Supplementary Figs. 3 and 4). This precaution avoids results driven by the large litterfall that occurs across these semi-deciduous forests during the dry season. Ultimately, the patterns and statistics remained largely unaffected by normalization to precipitation (i.e., statistically significant at $p < 0.1$), with correlation coefficients decreasing in some cases, but increasing in others. These steps were taken to ensure that we assessed soil effects on canopy properties independent from precipitation effects.

We assessed a large suite of soil variables and remote sensing products. Ultimately, the clearest results for the greenness analyses came from Landsat 8, which has the highest spatial resolution of all the products assessed. The high spatial resolution likely contributed to the ability to detect relatively clear patterns[107]. Though that is not to say that an improvement in spatial resolution for SIF or soil moisture would necessarily translate into stronger correlations; but, we had no ready way to test this[108]. We also tested the soil variables against MODIS NDVI, which has a coarser spatial resolution, but finer temporal resolution, than Landsat. Spatial resolution resulted in larger importance than temporal resolution in this particular analysis. This was likely due to the large spatial heterogeneity in soil properties in conjunction with the fortuitous acquisition of a sufficient number of cloud-free images from Landsat.

Given the significant coupling we found between *in situ* soil nutrients, soil C, and root biomass with remotely sensed canopy greenness limitation, we produced Panama-wide maps of soil C and N based on those respective

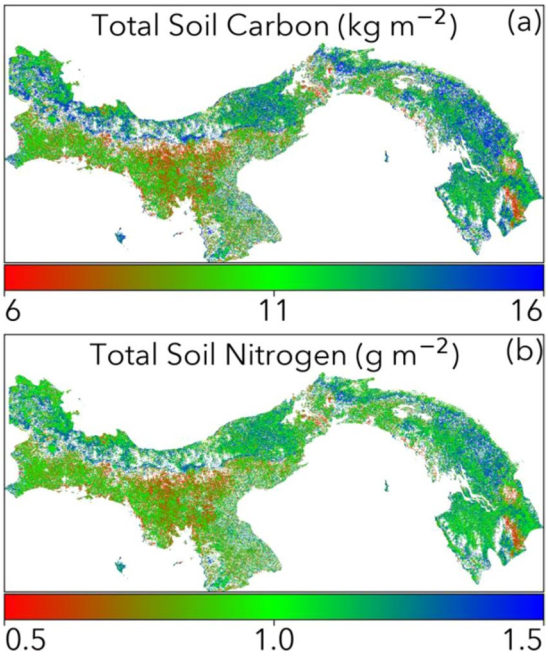

Figure 5. Panama-wide maps of (**a**) soil carbon and (**b**) nitrogen derived from plot-level relationships between soil measurements and satellite remotely sensed canopy properties. Reference uncertainty is 19% for soil carbon and 18% for soil nitrogen.

relationships (Fig. 5). We note that the maps should be treated more as thought exercises than as definitive truth, relying both on assumptions about the representativeness of the plots to the region/country at large as well as the soil-canopy relationships. For example, some areas are inaccessible and not well sampled by the plots, and are unlikely to be representative of the actual soil nutrients. As a reference for uncertainty in the maps, the linear model RMSE divided by plot mean was 19% for soil carbon and 18% for soil N. Given these caveats, some interesting spatial patterns do emerge. Total soil C and N are relatively well-constrained, with maxima along the Caribbean side and minima along the Cordillera de Talamanca mountain range. Interestingly, these maps compare (qualitatively) similarly to existing soils maps for the country[109–111]. There is potential power in many of these maps, as tropical soil C, for example, represents a large uncertainty in global C cycle models[112,113].

Conclusions

We found significant coupling between remotely sensed canopy properties of greenness and productivity with *in situ* soil nutrients, C, and toxic elements for humid tropical forests across soil fertility and precipitation gradients. These patterns emerged across a two-fold increase in precipitation, but relationships of canopy properties with soil nutrients were as strong or stronger than relationships with precipitation, providing new insight into how we think about canopy scale assessments of tropical ecosystem fertility and productivity. Soil nutrients led to competing effects on canopy greenness, with P and cations leading to a decrease in greenness related to increases litterfall, likely related to decreased nutrient use efficiency. In contrast, soil N corresponded to increased canopy greenness, and no relationship with litterfall. Of particular interest was the use of a novel remote sensing index of canopy greenness limitation, which we found had strong relationships with soil N, soil C, and root biomass, highlighting the potential utility of a remote sensing product for assessing belowground nutrients and C storage in some tropical ecosystems. Future satellite missions using imaging spectroscopy, for example, may further refine these analyses, disentangling much of the canopy chemistry differences related to soil nutrient patterns[114,115]. These results may help explain interpretations of the greening of the tropics due to CO_2 under nutrient limitations, and how climate projections and C cycle uncertainties are tied directly both to tropical ecosystem process understanding and soil carbon and nutrients.

Received: 26 September 2019; Accepted: 28 March 2020;
Published online: 21 April 2020

References

1. Schimel, D. *et al.* Observing terrestrial ecosystems and the carbon cycle from space. *Global Change Biology* **21**, 1762–1776 (2015).
2. Pan, Y. *et al.* A large and persistent carbon sink in the world's forests. *Science* **333**, 988–993, https://doi.org/10.1126/science.1201609 (2011).
3. Beer, C. *et al.* Terrestrial gross carbon dioxide uptake: Global distribution and covariation with climate. *Science* **329**, 834–838 (2010).
4. Malhi, Y., Gardner, T. A., Goldsmith, G. R., Silman, M. R. & Zelazowski, P. Tropical forests in the Anthropocene. *Annual Review of Environment and Resources* **39**, 125–159 (2014).
5. Sitch, S. *et al.* Recent trends and drivers of regional sources and sinks of carbon dioxide. *Biogeosciences* **12**, 653–679 (2015).

6. Huntzinger, D. N. *et al*. Uncertainty in the response of terrestrial carbon sink to environmental drivers undermines carbon-climate feedback predictions. *Scientific Reports* **7**, 1–8 (2017).
7. Schimel, D., Stephens, B. B. & Fisher, J. B. Effect of increasing CO2 on the terrestrial carbon cycle. *Proceedings of the National Academy of Sciences USA* **112**, 436–441, https://doi.org/10.1073/pnas.1407302112 (2015).
8. Cox, P. M. *et al*. Sensitivity of tropical carbon to climate change constrained by carbon dioxide variability. *Nature* **494**, 341–344, http://www.nature.com/nature/journal/v494/n7437/abs/nature11882.html#supplementary-information (2013).
9. Sellers, P. J., Schimel, D. S., Moore, B., Liu, J. & Eldering, A. Observing carbon cycle–climate feedbacks from space. *Proceedings of the National Academy of Sciences* **115**, 7868–7868, https://doi.org/10.1073/pnas.1716613115 (2018).
10. Zhu, Z. *et al*. Greening of the Earth and its drivers. *Nature Climate Change* **6**, 791–795 (2016).
11. Huete, A. R. *et al*. Amazon rainforests green-up with sunlight in dry season. *Geophysical Research Letters* **33**, 1–4 (2006).
12. Galvão, L. S. *et al*. On intra-annual EVI variability in the dry season of tropical forest: A case study with MODIS and hyperspectral data. *Remote Sensing of Environment* **115**, 2350–2359 (2011).
13. Lopes, A. P. *et al*. Leaf flush drives dry season green-up of the Central Amazon. *Remote Sensing of Environment* **182**, 90–98 (2016).
14. Saleska, S. R. *et al*. Dry-season greening of Amazon forests. *Nature* **531**, E4–E5 (2016).
15. Asner, G. P. & Alencar, A. Drought impacts on the Amazon forest: the remote sensing perspective. *New Phytologist* **187**, 569–578, https://doi.org/10.1111/j.1469-8137.2010.03310.x (2010).
16. Nemani, R. R. *et al*. Climate-driven increases in global terrestrial net primary production from 1982 to 1999. *Science* **300**, 1560–1563 (2003).
17. Elser, J. J. *et al*. Global analysis of nitrogen and phosphorus limitation of primary producers in freshwater, marine and terrestrial ecosystems. *Ecology Letters* **10**, 1135–1142 (2007).
18. Quesada, C. A. *et al*. Basin-wide variations in Amazon forest structure and function are mediated by both soils and climate. *Biogeosciences* **9**, 2203–2246, https://doi.org/10.5194/bg-9-2203-2012 (2012).
19. Fisher, J. B., Badgley, G. & Blyth, E. Global nutrient limitation in terrestrial vegetation. *Global Biogeochemical Cycles* **26**, GB3007, https://doi.org/10.1029/2011GB004252 (2012).
20. Vitousek, P. M. Litterfall, nutrient cycling, and nutrient limitation in tropical forests. *Ecology* **65**, 285–298 (1984).
21. Cleveland, C. C. *et al*. Relationships among net primary productivity, nutrients and climate in tropical rain forest: a pan-tropical analysis. *Ecology Letters* **14**, 939–947 (2011).
22. Townsend, A. R., Cleveland, C. C., Houlton, B. Z., Alden, C. B. & White, J. W. Multi-element regulation of the tropical forest carbon cycle. *Frontiers in Ecology and the Environment* **9**, 9–17 (2011).
23. Wright, S. J. Plant responses to nutrient addition experiments conducted in tropical forests. *Ecological Monographs* **89**, 1–18 (2019).
24. Cleveland, C. C., Townsend, A. R. & Schmidt, S. K. Phosphorus Limitation of Microbial Processes in Moist Tropical Forests: Evidence from Short-term Laboratory Incubations and Field Studies. *Ecosystems* **5**, 680–691, https://doi.org/10.1007/s10021-002-0202-9 (2002).
25. Vitousek, P. M., Porder, S., Houlton, B. Z. & Chadwick, O. A. Terrestrial phosphorus limitation: mechanisms, implications, and nitrogen–phosphorus interactions. *Ecological Applications* **20**, 5–15, https://doi.org/10.1890/08-0127.1 (2010).
26. Herbert, D. A. & Fownes, J. H. Phosphorus limitation of forest leaf area and net primary production on a highly weathered soil. *Biogeochemistry* **29**, 223–235 (1995).
27. Yang, X., Thornton, P., Ricciuto, D. & Post, W. The role of phosphorus dynamics in tropical forests–a modeling study using CLM-CNP. *Biogeosciences* **11**, 1667–1681 (2014).
28. McGroddy, M., Silver, W., De Oliveira, R., De Mello, W. & Keller, M. Retention of phosphorus in highly weathered soils under a lowland Amazonian forest ecosystem. *Journal of Geophysical Research: Biogeosciences* **113**, 1–11 (2008).
29. Reich, P. B. & Oleksyn, J. Global patterns of plant leaf N and P in relation to temperature and latitude. *Proceedings of the National Academy of Sciences* **101**, 11001–11006, https://doi.org/10.1073/pnas.0403588101 (2004).
30. Turner, B. L., Brenes-Arguedas, T. & Condit, R. Pervasive phosphorus limitation of tree species but not communities in tropical forests. *Nature* **555**, 367–370 (2018).
31. LeBauer, D. S. & Treseder, K. K. Nitrogen limitation of net primary productivity in terrestrial ecosystems is globally distributed. *Ecology* **89**, 371–379 (2008).
32. Matson, P. A., McDowell, W. H., Townsend, A. R. & Vitousek, P. M. The globalization of N deposition: ecosystem consequences in tropical environments. *Biogeochemistry* **46**, 67–83 (1999).
33. Vitousek, P. M. & Howarth, R. W. Nitrogen limitation on land and in the sea: How can it occur? *Biogeochemistry* **13**, 87–115 (1991).
34. Fisher, J. B. *et al*. Nutrient limitation in rainforests and cloud forests along a 3,000-m elevation gradient in the Peruvian Andes. *Oecologia* **172**, 889–902, https://doi.org/10.1007/s00442-012-2522-6 (2013).
35. Davidson, E. A. *et al*. Nitrogen and phosphorus limitation of biomass growth in a tropical secondary forest. *Ecological Applications* **14**, 150–163 (2004).
36. Cusack, D. F., Silver, W. L., Torn, M. S. & McDowell, W. H. Effects of nitrogen additions on above-and belowground carbon dynamics in two tropical forests. *Biogeochemistry* **104**, 203–225 (2011).
37. Wright, S. J. *et al*. Potassium, phosphorus, or nitrogen limit root allocation, tree growth, or litter production in a lowland tropical forest. *Ecology* **92**, 1616–1625, https://doi.org/10.1890/10-1558.1 (2011).
38. Powers, J. S. & Salute, S. Macro-and micronutrient effects on decomposition of leaf litter from two tropical tree species: inferences from a short-term laboratory incubation. *Plant and Soil* **346**, 245–257 (2011).
39. Yavitt, J. B., Harms, K. E., Garcia, M. N., Mirabello, M. J. & Wright, S. J. Soil fertility and fine root dynamics in response to 4 years of nutrient (N, P, K) fertilization in a lowland tropical moist forest, Panama. *Austral Ecology* **36**, 433–445 (2011).
40. Bern, C. R., Townsend, A. R. & Farmer, G. L. Unexpected dominance of parent-material strontium in a tropical forest on highly weathered soils. *Ecology* **86**, 626–632 (2005).
41. Baribault, T. W., Kobe, R. K. & Finley, A. O. Tropical tree growth is correlated with soil phosphorus, potassium, and calcium, though not for legumes. *Ecological Monographs* **82**, 189–203 (2012).
42. Cusack, D. F. *et al*. Global change effects on humid tropical forests: Evidence for biogeochemical and biodiversity shifts at an ecosystem scale. *Reviews of Geophysics* **54**, 523–610 (2016).
43. Cusack, D. F., Markesteijn, L., Condit, R., Lewis, O. T. & Turner, B. L. Soil carbon stocks across tropical forests of Panama regulated by base cation effects on fine roots. *Biogeochemistry* **137**, 253–266 (2018).
44. Kaspari, M. *et al*. Multiple nutrients limit litterfall and decomposition in a tropical forest. *Ecology Letters* **11**, 35–43, https://doi.org/10.1111/j.1461-0248.2007.01124.x (2008).
45. Townsend, A. R., Cleveland, C. C., Asner, G. P. & Bustamante, M. M. C. Controls over foliar N:P ratios in tropical rain forests. *Ecology* **88**, 107–118, https://doi.org/10.1890/0012-9658(2007)88[107:cofnri]2.0.co;2 (2007).
46. Malhi, Y. & Phillips, O. L. Tropical forests and global atmospheric change: a synthesis. *Philosophical Transactions of the Royal Society of London B: Biological Sciences* **359**, 549–555 (2004).
47. Zhao, M. S., Heinsch, F. A., Nemani, R. R. & Running, S. W. Improvements of the MODIS terrestrial gross and net primary production global data set. *Remote Sensing of Environment* **98**, 164–176 (2005).
48. Fisher, J. B. *et al*. Tree-mycorrhizal associations detected remotely from canopy spectral properties. *Global Change Biology* **22**, 2596–2607, https://doi.org/10.1111/gcb.13264 (2016).

49. Fisher, J. B. *et al*. The future of evapotranspiration: Global requirements for ecosystem functioning, carbon and climate feedbacks, agricultural management, and water resources. *Water Resources Research* **53**, 2618–2626, https://doi.org/10.1002/2016WR020175 (2017).
50. Schaaf, C. B. *et al*. First operational BRDF, albedo nadir reflectance products from MODIS. *Remote Sensing of Environment* **83**, 135–148 (2002).
51. Hulley, G. C. & Hook, S. J. Generating consistent land surface temperature and emissivity products between ASTER and MODIS data for earth science research. *Geoscience and Remote Sensing, IEEE Transactions on* **49**, 1304–1315 (2011).
52. Engelbrecht, B. M. *et al*. Drought sensitivity shapes species distribution patterns in tropical forests. *Nature* **447**, 80–82 (2007).
53. Condit, R., Engelbrecht, B. M., Pino, D., Pérez, R. & Turner, B. L. Species distributions in response to individual soil nutrients and seasonal drought across a community of tropical trees. *Proceedings of the National Academy of Sciences* **110**, 5064–5068 (2013).
54. Turner, B. L. & Engelbrecht, B. M. Soil organic phosphorus in lowland tropical rain forests. *Biogeochemistry* **103**, 297–315 (2011).
55. Pyke, C. R., Condit, R., Aguilar, S. & Lao, S. Floristic composition across a climatic gradient in a neotropical lowland forest. *Journal of Vegetation Science* **12**, 553–566 (2001).
56. Windsor, D., Rand, A. & Rand, W. Caracteristicas de la precipitacion en la isla de Barro Colorado. *Ecología de un bosque tropical: ciclos estacionales y cambios a largo plazo. Smithsonian Tropical Research Institute, Balboa*, 53-71 (1990).
57. Xie, P. & Arkin, P. A. Global monthly precipitation estimates from satellite-observed outgoing longwave radiation. *Journal of Climate* **11**, 137–164 (1998).
58. Medvigy, D. & Beaulieu, C. Trends in daily solar radiation and precipitation coefficients of variation since 1984. *Journal of Climate* **25**, 1330–1339 (2012).
59. Liebmann, B. *et al*. A comparison of rainfall, outgoing longwave radiation, and divergence over the Amazon Basin. *Journal of Climate* **11**, 2898–2909 (1998).
60. Turner, B. L., Yavitt, J. B., Harms, K. E., Garcia, M. N. & Wright, S. J. Seasonal changes in soil organic matter after a decade of nutrient addition in a lowland tropical forest. *Biogeochemistry* **123**, 221–235 (2015).
61. Stewart, R. & Stewart, J. Geologic map of the Panama Canal and vicinity, Republic of Panama (1980).
62. Woodring, W. P. Geology of Barro Colorado Island, Canal Zone (1958).
63. Chave, J. *et al*. Error propagation and scaling for tropical forest biomass estimates. *Philosophical Transactions of the Royal Society of London B: Biological Sciences* **359**, 409–420 (2004).
64. Roy, D. P. *et al*. Landsat-8: Science and product vision for terrestrial global change research. *Remote Sensing of Environment* **145**, 154–172 (2014).
65. Liang, S. Numerical experiments on the spatial scaling of land surface albedo and leaf area index. *Remote Sensing Reviews* **19**, 225–242 (2000).
66. Zanter, K. Landsat 8 (L8) data users handbook. *Landsat Science Official Website. Available online*, https://landsat.usgs.gov/landsat-8-l8-data-users-handbook (*accessed on 20 January 2018*) (2016).
67. Justice, C. *et al*. An overview of MODIS Land data processing and product status. *Remote Sensing of Environment* **83**, 3–15 (2002).
68. Entekhabi, D. *et al*. The Soil Moisture Active Passive (SMAP) Mission. *Proceedings of the IEEE* **98**, 704–716, https://doi.org/10.1109/JPROC.2010.2043918 (2010).
69. Frankenberg, C. *et al*. Prospects for chlorophyll fluorescence remote sensing from the Orbiting Carbon Observatory-2. *Remote Sensing of Environment* **147**, 1–12 (2014).
70. Sun, Y. *et al*. OCO-2 advances photosynthesis observation from space via solar-induced chlorophyll fluorescence. *Science* **358**, eaam5747 (2017).
71. Simard, M., Pinto, N., Fisher, J. B. & Baccini, A. Mapping forest canopy height globally with spaceborne lidar. *J. Geophys. Res.* **116**, 1–12, https://doi.org/10.1029/2011jg001708 (2011).
72. Pearlman, J. S. *et al*. Hyperion, a space-based imaging spectrometer. *IEEE Transactions on Geoscience and Remote Sensing* **41**, 1160–1173 (2003).
73. Huete, A. R., Liu, H. & van Leeuwen, W. J. In *Geoscience and Remote Sensing, 1997. IGARSS'97. Remote Sensing-A Scientific Vision for Sustainable Development., 1997 IEEE International*. 1966-1968 (IEEE).
74. Asner, G. P., Scurlock, J. M. & A. Hicke, J. Global synthesis of leaf area index observations: implications for ecological and remote sensing studies. *Global Ecology and Biogeography* **12**, 191–205 (2003).
75. Dent, D. H., Bagchi, R., Robinson, D., Majalap-Lee, N. & Burslem, D. F. Nutrient fluxes via litterfall and leaf litter decomposition vary across a gradient of soil nutrient supply in a lowland tropical rain forest. *Plant and Soil* **288**, 197–215 (2006).
76. Sayer, E. J. & Tanner, E. V. Experimental investigation of the importance of litterfall in lowland semi-evergreen tropical forest nutrient cycling. *Journal of Ecology* **98**, 1052–1062 (2010).
77. Wright, S. J. *et al*. Plant responses to fertilization experiments in lowland, species-rich, tropical forests. *Ecology* **99**, 1129–1138 (2018).
78. Sellers, P. J. Canopy reflectance, photosynthesis and transpiration. *International Journal of Remote Sensing* **6**, 1335–1372 (1985).
79. Carlson, T. N. & Ripley, D. A. On the relation between NDVI, fractional vegetation cover, and leaf area index. *Remote Sensing of Environment* **62**, 241–252 (1997).
80. Powers, J. S. & Schlesinger, W. H. Relationships among soil carbon distributions and biophysical factors at nested spatial scales in rain forests of northeastern Costa Rica. *Geoderma* **109**, 165–190 (2002).
81. Cronan, C. S. & Grigal, D. F. Use of calcium/aluminum ratios as indicators of stress in forest ecosystems. *Journal of Environmental Quality* **24**, 209–226 (1995).
82. Rustad, L. E. & Cronan, C. S. Cycling of aluminum and nutrients in litterfall of a red spruce (Picea rubens Sarg.) stand in Maine. *Canadian Journal of Forest Research* **19**, 18–23 (1989).
83. Poschenrieder, C., Gunsé, B., Corrales, I. & Barceló, J. A glance into aluminum toxicity and resistance in plants. *Science of the Total Environment* **400**, 356–368 (2008).
84. Roy, A. K., Sharma, A. & Talukder, G. Some aspects of aluminum toxicity in plants. *The Botanical Review* **54**, 145–178 (1988).
85. Foy, C., Chaney, R. T. & White, M. The physiology of metal toxicity in plants. *Annual Review of Plant Physiology* **29**, 511–566 (1978).
86. Delhaize, E. & Ryan, P. R. Aluminum toxicity and tolerance in plants. *Plant Physiology* **107**, 315–321 (1995).
87. Ribeiro, M. A. Q. *et al*. Aluminum effects on growth, photosynthesis, and mineral nutrition of Cacao genotypes. *J. Plant Nutr.* **36**, 1161–1179, https://doi.org/10.1080/01904167.2013.766889 (2013).
88. Zemunik, G., Davies, S. J. & Turner, B. L. Soil drivers of local-scale tree growth in a lowland tropical forest. *Ecology* **99**, 2844–2852, https://doi.org/10.1002/ecy.2532 (2018).
89. Kochian, L. V., Hoekenga, O. A. & Pineros, M. A. How do crop plants tolerate acid soils? Mechanisms of aluminum tolerance and phosphorous efficiency. *Annu. Rev. Plant Biol.* **55**, 459–493 (2004).
90. Ren, H. *et al*. The role of autophagy in alleviating damage of aluminum stress in Arabidopsis thaliana. *Plant Growth Regul.* **79**, 167–175, https://doi.org/10.1007/s10725-015-0122-2 (2016).
91. Chapin, F. S. III, Vitousek, P. M. & Cleve, K. V. The nature of nutrient limitation in plant communities. *The American Naturalist* **127**, 48–58 (1986).
92. Attiwill, P. M. & Adams, M. A. Nutrient cycling in forests. *New Phytologist* **124**, 561–582 (1993).

93. McGroddy, M. E., Daufresne, T. & Hedin, L. O. Scaling of C:N:P Stoichiometry in Forests Worldwide: Implications of Terrestrial Redfield-Type Ratios. *Ecology* **85**, 2390–2401, https://doi.org/10.1890/03-0351 (2004).
94. Berg, B. & Laskowski, R. Litter fall. *Advances in Ecological Research* **38**, 19–71 (2005).
95. Phillips, R. P., Erlitz, Y., Bier, R. & Bernhardt, E. S. New approach for capturing soluble root exudates in forest soils. *Functional Ecology* **22**, 990–999 (2008).
96. Fisher, J. B., Huntzinger, D. N., Schwalm, C. R. & Sitch, S. Modeling the terrestrial biosphere. *Annual Review of Environment and Resources* **39**, 91–123 (2014).
97. Allen, K. E., Fisher, J. B., R.P., P., Power, J. & Brzostek, E. R. Modeling the carbon cost of plant nitrogen and phosphorus uptake across temperate and tropical forests. *Frontiers in Forests and Global Change*, in press (2020).
98. Fleischer, K. *et al*. Amazon forest response to CO 2 fertilization dependent on plant phosphorus acquisition. *Nature Geoscience* **12**, 736–741 (2019).
99. Chambers, J. *et al*. Next Generation Ecosystem Experiment (NGEE) Tropics. *US DOE NGEE Tropics White Paper* (2014).
100. Luo, Y. *et al*. A framework for benchmarking land models. *Biogeosciences* **9**, 3857–3874, https://doi.org/10.5194/bg-9-3857-2012 (2012).
101. Kelley, D. I. *et al*. A comprehensive benchmarking system for evaluating global vegetation models. *Biogeosciences* **10**, 3313–3340, https://doi.org/10.5194/bg-10-3313-2013 (2013).
102. Fisher, J. B. *et al*. The land-atmosphere water flux in the tropics. *Global Change Biology* **15**, 2694–2714 (2009).
103. Polhamus, A., Fisher, J. B. & Tu, K. P. What controls the error structure in evapotranspiration models? *Agricultural and Forest Meteorology* **169**, 12–24, https://doi.org/10.1016/j.agrformet.2012.10.002 (2013).
104. Fisher, J. B. *et al*. ECOSTRESS: NASA's next generation mission to measure evapotranspiration from the International Space Station. *Water Resources Research*, in press (2020).
105. Santiago, L. S., Schuur, E. A. & Silvera, K. Nutrient cycling and plant–soil feedbacks along a precipitation gradient in lowland Panama. *Journal of Tropical Ecology* **21**, 461–470 (2005).
106. Posada, J. M. & Schuur, E. A. Relationships among precipitation regime, nutrient availability, and carbon turnover in tropical rain forests. *Oecologia* **165**, 783–795 (2011).
107. Bohlman, S. A. Landscape patterns and environmental controls of deciduousness in forests of central Panama. *Global Ecology and Biogeography* **19**, 376–385 (2010).
108. Colliander, A. *et al*. Spatial downscaling of SMAP soil moisture using MODIS land surface temperature and NDVI during SMAPVEX15. *IEEE Geoscience and Remote Sensing Letters* **14**, 2107–2111 (2017).
109. FAO-UNESCO. *The FAO-UNESCO Soil Map of the World*. (Food and Agriculture Organization of the United Nations, 1968).
110. Sanchez, P. A. *et al*. Digital soil map of the world. *Science* **325**, 680–681 (2009).
111. Nachtergaele, F. *et al*. In *Proceedings of the 19th World Congress of Soil Science*, *Soil Solutions for a Changing World, Brisbane, Australia, 1-6 August 2010*. 34-37.
112. Le Quéré, C., *et al*. Trends in the sources and sinks of carbon dioxide. *Nature Geosci* **2**, 831-836, http://www.nature.com/ngeo/journal/v2/n12/suppinfo/ngeo689_S1.html (2009).
113. Post, W. M., Emanuel, W. R., Zinke, P. J. & Stangenberger, A. G. Soil carbon pools and world life zones. *Nature* **298**, 156 (1982).
114. National Academies of Sciences, Engineering & Medicine. *Thriving on Our Changing Planet: A Decadal Strategy for Earth Observation from Space*. (The National Academies Press, 2018).
115. Higgins, M. A. *et al*. Linking imaging spectroscopy and LiDAR with floristic composition and forest structure in Panama. *Remote Sensing of Environment* **154**, 358–367 (2014).

Acknowledgements

The remote sensing analysis was carried out at the Jet Propulsion Laboratory, California Institute of Technology, under a contract with the National Aeronautics and Space Administration. California Institute of Technology. Government sponsorship acknowledged. Funding was provided by the National Science Foundation (NSF) Geography & Spatial Science (GSS) program (BCS-1437591; J.B.F., N.V.P., D.F.C.), Department of Energy (DOE) Office of Science Terrestrial Ecosystem Science (J.B.F.: DE-SC0016188; D.F.C.: Early Career Award DE-SC0015898), and NASA Interdisciplinary Science (IDS) and Terrestrial Ecology (TE) programs (J.B.F.). Copyright 2020. All rights reserved.

Author contributions

J.B.F. and D.F.C. formulated idea; J.B.F. designed research; J.B.F. and N.V.P. performed research; D.F.C. and B.T. provided data; J.B.F., N.V.P., B.T., D.S.S., and D.F.C. contributed to the writing of the paper.

Competing interests

The authors declare no competing interests.

Additional information

Supplementary information is available for this paper at https://doi.org/10.1038/s41598-020-63589-1.

Correspondence and requests for materials should be addressed to J.B.F.

Reprints and permissions information is available at www.nature.com/reprints.

Publisher's note Springer Nature remains neutral with regard to jurisdictional claims in published maps and institutional affiliations.